Published in final edited form as:
J Control Release. 2010 March 19; 142(3): 332–338. doi:10.1016/j.jconrel.2009.11.007.

Lesion Complexity Determines Arterial Drug Distribution After Local Drug Delivery

Abraham R. Tzafriri, Ph.D.[a], **Neda Vukmirovic, Ph.D.**[a], **Vijaya B. Kolachalama, Ph.D.**[a], **Irina Astafieva, Ph.D.**[b], and **Elazer R. Edelman, M.D., Ph.D., FACC**[a,c]

[a]Harvard-MIT Division of Health Sciences and Technology, Massachusetts Institute of Technology, Cambridge, Massachusetts 02139

[b]Abbott Cardiovascular Systems, Santa Clara, California 95054

[c]Cardiovascular Division, Department of Medicine, Brigham and Women's Hospital, Harvard Medical School, Boston, Massachusetts 02115

Abstract

Though stents are deployed in diseased arteries drug distribution has only been quantified in intact, non-diseased vessels. We correlated steady-state arterial drug distribution with tissue ultrastructure and composition, in abdominal aortae from atherosclerotic human autopsy specimens and rabbits with lesions induced by dietary manipulation and controlled injury. Paclitaxel, everolimus, and sirolimus deposition in human aortae was maximal in the media and scaled inversely with lipid content. Net tissue paclitaxel and everolimus levels were indistinguishable in mildly injured rabbit arteries independent of diet. Yet, serial sectioning of cryopreserved arterial segments demonstrated a differential transmural deposition pattern that was amplified with disease and correlated with expression of their intracellular targets, tubulin and FKBP-12. Tubulin distribution and paclitaxel binding increased with vascular injury and macrophage infiltration, and were reduced with lipid content. Sirolimus analogues and their specific binding target FKBP-12 were less sensitive to alterations of diet in mildly injured arteries, presumably reflecting a faster transient response of FKBP-12 to injury. The data demonstrate that disease-induced changes in the distribution of drug binding proteins and interstitial lipid alter the distribution of these drugs, forcing one to consider how disease might affect the evaluation and efficacy of local release of these and like compounds.

Keywords

Arteries; Drugs; Lesion; Pharmacokinetics; Stents

Correspondence should be addressed to: Abraham Rami Tzafriri, Division of Health Sciences and Technology, Massachusetts Institute of Technology, Room E25-449, 77 Massachusetts Avenue, Cambridge, Massachusetts 02139, Phone: (617) 252-1655, Fax: (617) 253-2514, ramitz@mit.edu.
The first 2 authors contributed equally to this article.

INTRODUCTION

Local drug delivery from endovascular stents has transformed how we treat coronary artery disease. Yet, few drugs are in fact effective when delivered from endovascular implants and those that possess a narrow therapeutic window. The width of this window is predicated to a great degree upon the extent of drug deposition and distribution through the arterial wall(1–5). Drugs that are retained within the blood vessel are far more effective than those that are not(5). Thus, for example, heparin regulates virtually every aspect of the vascular response to injury(6), yet is so soluble and diffusible that it simply cannot stay in the artery for more than minutes after release. Heparin therefore has no effect on intimal hyperplasia when eluted from a stent(3,4). Paclitaxel and sirolimus in contradistinction are far smaller compounds with perhaps more narrow and specific effects than heparin. Yet, these drugs bind tenaciously to tissue protein elements and specific intracellular targets(7–9) and remain beneath stent struts long after release(10,11). The clinical efficacy of paclitaxel and sirolimus at reducing coronary artery restenosis rates following elution from stents appears incontrovertible(12,13). However, emerging clinical and preclinical data suggest that the benefit of the local release of these drugs is beset by significant complications, that rise with lesion complexity(14–16), e.g. as the native composition and layered ultrastructure of the native artery is more significantly disrupted. It has been suggested that the compositional changes in the artery that accompany increased atherosclerosis affect local tissue capacity for drug absorption and retention as well as the biologic response to injury and pharmacologic response to the drug(14). In contrast to such lesion capacitance effects, local thrombotic response to stent deployment can also affect arterial drug distribution by forming a mural layer that impedes drug penetration into target lesions(17,18).

Thus, Virmani and others have hypothesized that the attraction of lipophilic drugs like paclitaxel and sirolimus to fat should affect their retention within and effects upon atheromatous lesions(14). None-the-less, this aspect of drug delivery has not been tested as the bulk of preclinical studies to date have utilized intact, normal arteries and animals. We now examine the spatial distribution and net compartmental deposition of paclitaxel and sirolimus analogs in diseased arteries, human autopsy samples and controlled animal models of disease and injury. Local deposition of these drugs correlated with local arterial composition, falling with increasing local lipid and cholesterol contents and highlighting that tissue deposition for locally delivered drugs is dominated by binding to intracellular and matrix proteins(7–9), not simply by lipophilic partitioning effects. As tissue binding capacities are independent of the mode of delivery, our results are of general relevance to endovascular drug delivery, and of particular significance to delivery from coated balloons(19,20). In the latter, large doses of drug are delivered by direct contact with the artery over periods of seconds to minutes, with minimal dilution by flowing blood; sustained tissue retention and efficacy then depend critically on drugtissue interactions(21,22).

METHODS

Model Drugs

Labeled analogs of three clinically relevant model drugs were employed, Paclitaxel (854 Da), Sirolimus (914 Da), and the Sirolimus analog, Everolimus (958 Da). H^3-labeled Paclitaxel was obtained from Vitrax (Placentia, CA), H^3-labeled Everolimus was a gift from the Guidant Corporation (Santa Monica, CA) and C^{14}-labeled Sirolimus was a gift from Cordis, a division of Johnson&Johnson. The cell permeable fluorescent Paclitaxel analog (TubulinTracker™ Green, 1403 Da) was purchased from Molecular Probes (Eugene, OR).

Arterial Samples

Tissues were obtained from three related arterial beds with variable degrees of atherosclerosis, including abdominal aortae from human autopsy specimens, and rabbit aortae subject to an extended period of high fat dietary intake.

Human—Sections of the abdominal aorta from four humans were obtained within 24 hours of demise from the Pathology department of the Brigham and Women's Hospital (Boston, MA) under institutional guidelines that precluded access to patient specific data. Histological characterization confirmed that vessels displayed a range of lesions, but all contained modest to significant lipid deposits, but no thrombi, and scattered areas of necrosis or calcifications. After cleaning, one artery sample was immunostained to examine tissue preservation and ultrastructure, two artery samples were used for studying bulk equilibrium drug uptake, one sample was separated into tunica layers and used to assess compartmental drug loadings and cholesterol contents.

Rabbit—Atheromatous and atherosclerotic lesions were induced in the aortae and iliac arteries of New Zealand White Rabbits through control of diet and catheter induced vascular injury. Ten male rabbits, weighing 3.0–3.5kg, approximately 3 months old, were fed a normal (n=5) or high cholesterol/high fat diet (n=5, 2% cholesterol and 6% peanut oil) for 4 weeks and injured at 2 weeks with 3F Fogarty balloon-tipped catheters (3F Fogarty Arterial Embolectomy catheter, Edwards Lifesciences). Two different balloon-tipped catheters were employed to provide two different degrees of injury - the first a 1cc, 40 mm and the second 0.5cc 20 mm. Each balloon was inflated to its full extent and withdrawn along the length of the artery. Six rabbits, three from each diet group, were catheter injured at a low inflation volume (0.5cc), sacrificed at 4 weeks and the injured artery harvested fresh without pressure or perfusion. Arteries from these animals exhibited non-uniform lipid infiltration and were atheromatous in nature. In the remaining animals (n=4) injury at two weeks was induced with higher inflation volumes (1.0cc). In these animals normal diet was resumed at the end of 4 weeks for approximately 4 additional months and tissues then harvested. Animals that were maintained for 4 additional months after high fat diet and denuding injury developed more sclerotic lesions. While arteries from the former animals were lipid infiltrated those from the latter animals exhibited far greater degrees of sclerosis and changes in elastin, collagen and calcium, as well as, lipid content. The calcified nature of these lesions precluded their enface cryosectioning for transmural distribution, but allowed for serial transverse sectioning with precise maintenance of tissue architecture and alignment. This enabled *in situ* correlation of drug distribution and lesion content. The use of fluorescent imaging restricted our analysis to paclitaxel for which well characterized commercial fluorescent analogs are available.

Partition coefficient and drug distribution

Net and compartmental partition coefficients—We defined the equilibrium net arterial and compartmental partition coefficients of radiolabeled paclitaxel, everolimus, and sirolimus in aqueous buffered saline solutions of drug. Square (4mm×4mm) arterial segments were weighed before being placed in drug bath solutions at room temperature for 0–96 h and then processed in triplicate for liquid scintillation counting. Normalization of the scintillation counts to tissue mass yielded a drug concentration for each tissue sample (c_T) that was further normalized to the corresponding drug concentration in the bulk fluid (c_{bulk}) to determine the net arterial partition coefficient (K)

$$K = c_T / c_{bulk}. \quad [1]$$

For evaluation of the compartmental partition coefficient of human arteries, aortae were separated into the three tunical compartments and the partition coefficient evaluated as for the whole artery samples. Consistency in tissue density was ensured by employing only lightly calcified arterial segments in drug partitioning studies. 2% PEG-200 were added to all everolimus solutions to ensure its stability in the aqueous environment. Normalized uptake transients were fit to mono-exponential kinetics, yielding estimates of the apparent rate constant of drug uptake and the fraction of retained drug.

Transmural distribution of drug partitioning—Equilibrated transmural drug distributions were measured through enface cryosectioning. Arterial segments were incubated in the drug bath for 48 h, and then laid flat and snap-frozen in a plastic encasement with Tissue-Tek OCT compound (Sakura Finetechnical, Tokyo). Segment length and width were measured with digital calipers before freezing. Samples were stored in a −80°C freezer until they were sectioned parallel to the intima(23–25) with a refrigerated microtome (Cryotome SME, Shandon, Pittsburgh). Sections 0.020 mm thick were cut parallel to the intima, and the drug content of each sample was determined by liquid scintillation spectroscopy. The partition coefficient at each transmural location x was calculated as the mass of drug normalized by the measured tissue area and slice thickness ($c_T(x)$) and by the equilibrium bulk fluid drug concentration c_{bulk},

$$K(x)=c_T(x)/c_{bulk} \quad [2]$$

Fluorescent drug distribution—Fluorescent drug distribution was determined in a similar manner. After prescribed incubations with labeled drug, tubular arterial segments were removed from binding media, washed with buffer, snap frozen and embedded in tissue freezing medium (OCT) cryosectioned to yield 0.010 mm thick parallel cross-sections with a cryostat (Shandon, Inc), and prepared for fluorescent microscopy or immunohistochemistry. The former were fixed in ice-cold paraformaldehyde (4%) for 10 minutes, rinsed in PBS, mounted and cover-slipped, and subsequently imaged on an epifluorescence microscope (Leica DMRA2 equipped with a Hamamatsu C4742-95 digital camera).

Correlation of fluorescent drug distribution with arterial composition

Arterial ultrastructure—was examined in frozen sections (lipid, elastin) or paraffin embedded sections (β-Tubulin and FKBP-12) adjacent to sections assayed for drug distribution. Cholesterol content of 4mm×4mm square tissue segments of human aorta was assayed in triplicate for each tunica layer using standard homogenation and cholesterol extraction techniques(26) and cholesterol quantification by an enzymatic method(27). Lipid distribution in rabbit aortae was defined with Oil-Red-O stain and elastin with verHoeff stain.

Correlation of fluorescent drug distribution and histological stains—was performed on serial sections using in house adaptations of imaging and computational alignment technologies(28–30). Digitized images were extracted in RGB space (MATLAB, Mathworks Inc.). The full dynamic range from absolute black (0,0,0) to absolute white (255,255,255) was used and a scalar value of pixel luminosity L(i,j) was determined as a weighted sum of the color values of each pixel, R(i,j), G(i,j) and B(i,j), using the Rec. 601 standard(31)

$$L(i,j)=0.299^{*}R(i,j)+0.587^{*}G(i,j)+0.114^{*}B(i,j). \quad [3]$$

Drug and compositional metrics were quantified and correlated at a compartmental level, in each of the tunica layers, or at an intra-compartmental level. All images were processed to eliminate backgrounds and artifacts, and pixel values between thresholds were extracted for all zones of interest. Specific algorithms analyzed each of the histo/immuno-stained arterial structures. Intra-compartmental analyses were performed by sub-dividing arterial cross-sections into 2–64 equal sectors and evaluating the pixel-average luminosity for each sector. Linear regression of drug versus compositional luminosities asymptotically approached steady state after subdivision into 16 sectors, as the effects of tissue processing on circumferential fluorescence were gradually filtered out. For compartmental correlation, each layer of the arterial wall was carefully cropped and aligned for comparison. The net changes in compartmental levels of drug and compositional elements were determined sequentially using image analysis techniques. The mean luminosities of the drug and each of the compositional elements were determined for each of the tunica layers from the appropriate images of control arteries. Subsequently, the percentages of pixels with luminosities above the mean in the respective control arteries were evaluated in control and diseased arteries, and changes induced by high fat diet evaluated as the difference between these two numbers.

Statistical analysis

Data are expressed as mean ± SE. Drug loading in control and disease groups was compared using the unpaired Student's *t* test. Differences were termed statistically significant at $p<0.05$. Non-linear regression was performed using Graphpad Prism 3.02 software to fit transient loading data to mono-exponential kinetics.

RESULTS

To examine lesion dependent morphological effects on the tissue binding capacities of paclitaxel and sirolimus analogs independent of stent design, we delivered drug via prolonged incubations in static drug binding media. This system controlled delivered dose and removed the significant unpredictability in release that is imposed by variability in stent position relative to the arterial wall, inflation techniques and stent geometry. As our steady state tissue distribution results were obtained under constant source conditions, without washout by flowing blood, they constitute upper bounds for arterial drug distribution following transient modes of in vivo drug delivery wherein only a fraction of the eluted dose is absorbed by the artery (32–34).

Human lesions

Immunostains of the human autopsy samples revealed a layered structure with smooth muscle cells and elastin primarily localized in the media, in contrast to lipid which distributed rather uniformly throughout the arterial wall (supplemental figure S1). The equilibrium partitioning of lipophilic drugs within the human abdominal aortae were estimated at the bulk and tunicae levels. The partition coefficient for paclitaxel in bulk normal segments of the aorta was 18.4 ± 0.8 and for the sirolimus analog 6.8 ± 0.4. These values fell 24.5% and 16.6% respectively ($p<0.05$, n=3) in aortic segments with high cholesterol content. When these tissues were dissected along tunic planes the dependence of drug uptake on tissue cholesterol content became even more apparent (Fig 1). The effect of lipid was greatest for paclitaxel, reducing peak drug deposition almost 3-fold as lipid content increased to its maximum ($p<0.0001$, $R=0.81$).

Atheromatous rabbit lesions

Rabbit models of controlled diets and vascular injury produced a more defined set of lesions in which to examine systematically the impact of lesion morphology on drug distribution

and net deposition. Arterial denudation injury with the low volume balloon catheters induced a thin neointima in all animals, but only the cholesterol/oil-enriched diet group (n=3) exhibited arterial lipid infiltrates. Net drug deposition into these arteries exhibited monoexponential kinetics (Fig 2A, R^2>0.65) with indistinguishable equilibrium partition coefficients (19.4 ± 1.4) and time constants (2.12 ± 0.7 h). All arteries exhibited bell-curve shaped drug profiles, but while disease altered the pattern of paclitaxel deposition (Fig 2B, p=0.08), everolimus patterns were independent of ultrastructural state (Fig 2C, p=0.37). Diseased arteries had a lower peak amount of paclitaxel, but maintained similar net drug contents as drug penetrated deeper into the vessel. The identity of kinetics and the similarities in distribution profiles speak to similar forces driving drug transport and retention(7), whereas quantitative differences reflect differential binding site densities.

Atherosclerotic rabbit lesions

Control abdominal aortae from animals subject to injury by a inflation with the higher capacity balloon catheters and 5 months of normal diet had scant lipid (Fig 3a), high levels of β-tubulin in the neointima but low levels in the media and the adventitia (Fig 3b), and a well defined internal elastic lamina but moderate elastin levels in the media and low levels in the neointima and adventitia (Fig 3c). Drug deposition (bright green in Fig 3d) was highest along the internal elastic lamina, high in the neointima, moderate in the media, and low in the adventitia. Thus, paclitaxel seems to associate within elastin-and microtubule-rich regions. Drug content fell 73±9% (Fig 3h) as the net lipid content rose 28±7% in diseased arteries (Fig 3e). The significant reduction in drug deposition associated with the intermittent fat-rich diet coincides with a marked increase in lipid within the neointima and media (Figs 3e) and a concomitant reduction in β-tubulin (Fig 3f) and elastin (Fig 3g) in these compartments. Thus, compartmental paclitaxel content seems to scale with tubulin and elastin contents but inversely with lipid (Fig 4). The relative absence of elastin and minimal presence of tubulin in these lesions allowed us to confirm and quantify the inverse linear correlation between local lipid and drug contents (Fig 5), similar to our findings in autopsy samples of human arteries (Fig 1).

DISCUSSION

There is much we do not yet know of drug-eluting stents and local vascular drug delivery. Questions remain as to when and why these devices function or potentially generate morbidity risk. There is not a clear understanding of how such devices function in acute thrombosis, chronic metabolic derangements like diabetes mellitus or vascular beds other than the coronary arteries. The literature suggests that efficacy of drug-eluting-stents is impacted by lesion complexity and degree of atherosclerosis (14–16,35,36). Similarly, emerging data infer that drug-eluting balloons can provide significant benefit to peripheral arterial disease when introduced at the time of direct intervention on existing complex lesions(37). The very efficacy of paclitaxel and sirolimus following local delivery is usually attributed to their lipophilicity(10) and sustained retention in the vessel wall compared to more hydrophilic compounds like heparin(21). It is hypothesized that deposition of lipophilic drugs will increase with arterial wall lipid content(14) and that drug effect should track with lesion composition and morphology. Yet, the bulk of preclinical studies to date have utilized intact arteries and normal animals and many of the postulates regarding tissue deposition have not been formally tested. The current study correlated drug distribution with local arterial composition in human autopsy samples and controlled animal models of arterial disease and injury and defied this hypothesis.

The distribution of three clinically relevant hydrophobic drugs in human autopsy samples revealed changes in drug distribution with lesion state, but in a manner that cannot be explained solely by drug lipophilicity or directly with arterial wall lipid content.

Remarkably, although all three drugs are hydrophobic, their compartmental deposition in the chronic atheromatous domains of the human aorta scaled inversely with compartmental cholesterol content (Fig 1; $p<0.0001$, $R=0.81$). Fresh calf carotid arteries had lower levels of cholesterol than the media of the human aorta samples, and correspondingly higher drug partition coefficients (supplemental figure S3).

More intricate effects were observed in controlled rabbit models that examined the compounded effects of diet and denudation on drug distribution following sustained drug incubation. The equilibrium deposition of paclitaxel and sirolimus-like drugs are differentially affected by lesion complexity. Whereas everolimus distribution in arteries that were injured at low catheter inflation volumes (0.5cc) was insensitive to differences in diet, paclitaxel distribution was significantly altered in animals that received a cholesterol rich diet (Fig 2), particularly in the subinitmal region. High levels of paclitaxel in the subintimal space of mildly injured arteries correlate with a diet-induced upregulation of tubulin in that area (supplemental Fig S4). Conversely, the apparent insensitivity of FKBP-12 distribution in mildly injured arteries to differences in diet (supplemental Fig S4) correlated with insignificant alterations in the distribution of sirolimus (Fig 2C). Catheter injury ar the higher inflation volume (1.0cc) allowed us to examine the correlation of paclitaxel distribution with lesion morphology and composition in the setting of greater vascular injury and ultimate tissue response. Acute disruption following local tissue damage removes natural transport barriers that hinder the accumulation of interstitial lipid, and induces an inflammatory stimulus that allows for marked increase in local accumulation of macrophages and dendritic cells(38–41). Levels of tubulin rise in injured arteries where hypercholesterolemia increases macrophage infiltration(42,43) and as suspected paclitaxel deposition increases in these local areas as well. Yet, there is also a reverse effect if interstitial lipid pools are dominant in place of macrophage infiltration. Lipid pools displace tubulin expressing cells in the intima and media, thereby removing a binding domain for paclitaxel (Figs 3 and 4), reducing its arterial deposition in a manner that scales inversely with lipid content (Fig 5). Notably, although tubulin expression was upregulated in the group of acutely injured arteries, diet abolished this effect (Fig 3), speaking to the reported differences in tubulin distribution.

Thus, it is only when binding to drug-specific tissue sites are added to transport considerations(44) that one can account for the differential deposition and distribution of drugs of near identical molecular weight, similar lipophilicity and solubility across similar arterial tissue. The differences in the dependence of drug deposition on tissue state may well represent the different balance each drug achieves between increased absorption of drug within macrophages and decreased binding in settings of lipid infiltration and cell displacement(42). Paclitaxel, by virtue of its effects on tubulin, effectively fixes macrophages in place(10,45) eliciting a mechanism for a cascade of injury, altered tissue state and affected local drug retention and perhaps effect. In contrast, sirolimus analogs were virtually unaffected by vascular manipulations (Fig 2), consistent with uniform, though low, expression of FKBP-12 in a range of arteries and transient upregulation of FKBP-12 that peaks early after and returns to baseline levels late after arterial injury(41,46). Intriguingly, macrophage infiltration does not chronically upregulate FKBP-12, suggesting a mechanism for differential effects of lesion complexity on the distribution and efficacy of paclitaxel and sirolimus analogs(14,47). While drug binding to specific intracellular targets is important, our finding of paclitaxel colocalization with elastin (Fig 3c,g), suggests that elastin displays a high binding capacity for paclitaxel, speaking to the importance of the extracellular matrix as a determinant of the distribution and retention of small hydrophobic drugs. In vitro imaging studies with tissue mimics also illustrated colocalization of fluorescent paclitaxel with elastin, and implicated the latter as a prime drug-binding substrate that impedes paclitaxel diffusion, rather than through steric hindrance(48).

LIMITATIONS

The idea that drug deposition after balloon inflation and stent implantation within diseased, atheromatous and sclerotic vessels tracks so precisely with specific tissue elements is an important consideration of drug-eluting technologies and may well require that we consider diseased rather than naïve tissues in preclinical evaluations. We must acknowledge that excised and autopsy specimens might undergo structural changes that we could not see after histological characterization, and that there are ultrastructural differences and different pathophysiologic consequences of disease in abdominal aorta and coronary arteries and between human and leporine tissues. Our use of abdominal aorta from human autopsy samples and rabbits subject to controlled diet and injury, rather than coronary arteries, ensured greater tissue preservation and allowed for comparison of like tissues in best preserved state. The immersion of tissues required for observing the differences we cite are not identical with drug elution from endovascular balloons, stents or perivascular wraps that specifically target a single aspect of the artery; immersion of tissue segments in binding medium allows for drug absorption not only from the intima and adventitia but also by lateral diffusion along the tunica layers. Nevertheless, the equilibrium effects that we report are essentially independent of such transport issues and are primarily a reflection of the tissue's equilibrium binding capacity for the drug.

CONCLUSIONS

The idea that the artery as a target tissue determines and regulates uptake of locally delivered drug is biologically appealing and consistent with concern raised as to the validity of evaluation of devices and drug-elution in preclinical animal models that employ normal blood vessels(14). Though animal models cannot predict human efficacy they can be used to test mechanism of action(49,50). When uninjured animal vessels are examined the extrapolation of mechanism to the clinical condition may be limited. The change in drug uptake and retention with tissue architecture and disease can begin to explain seemingly disparate findings from different clinical trials(15,16,35,36). It is only when drug binding to specific tissue sites is added to transport considerations(44) that one can account for the differential deposition and distribution of drugs of near identical molecular weight, similar lipophilicity and solubility across similar arterial tissue. Binding in turn requires an understanding of the kinetics of tissue response to injury. Indeed, the specific targets of the leading drugs eluted from stents, paclitaxel and sirolimus analogs, may express more abundantly in recruited inflammatory cells than in the native artery itself. Thus, the reaction of an artery first to the initial injury, then to the vascular repair and finally to the very effect of eluted drug will in turn influence drug absorption and distribution. It is in this way that different drugs can be absorbed by the same artery differently even at identical degrees of injury, cell infiltration and lipid insudation.

Supplementary Material

Refer to Web version on PubMed Central for supplementary material.

Acknowledgments

We are grateful for the support of Jacqueline Brazin, Adam Groothuis, Philip Seifert, Anna-Maria Spognardi, and David Wu. This work was supported in part by grants from the NIH (R01 GM 49039) and generous gifts of C^{14}-sirolimus and H^{3}-everolimus provided by Johnson and Johnson/Cordis and Guidant/Abbott Vascular.

REFERENCES

1. Hwang CW, Wu D, Edelman ER. Stent-based delivery is associated with marked spatial variations in drug distribution. Journal of the American College of Cardiology 2001;37:1a–2a. [PubMed: 11153722]
2. Hwang CW, Wu D, Edelman ER. Physiological transport forces govern drug distribution for stent-based delivery. Circulation 2001;104:600–605. [PubMed: 11479260]
3. Lovich MA, Brown L, Edelman ER. Drug clearance and arterial uptake after local perivascular delivery to the rat carotid artery. Journal of the American College of Cardiology 1997;29:1645–1650. [PubMed: 9180131]
4. Lovich MA, Edelman ER. Mechanisms of transmural heparin transport in the rat abdominal aorta after local vascular delivery. Circ Res 1995;77:1143–1150. [PubMed: 7586227]
5. Riessenand R, Isner JM. Prospects for site-specific delivery of pharmacologic and molecular therapies. Journal of the American College of Cardiology 1994;23:1234–1244. [PubMed: 8144794]
6. Nugent MA, Karnovsky MJ, Edelman ER. Vascular Cell-Derived Heparan-Sulfate Shows Coupled Inhibition of Basic Fibroblast Growth-Factor Binding and Mitogenesis in Vascular Smooth-Muscle Cells. Circulation Research 1993;73:1051–1060. [PubMed: 8222077]
7. Levin AD, Jonas M, Hwang CW, Edelman ER. Local and systemic drug competition in drug-eluting stent tissue deposition properties. J Control Release 2005;109:236–243. [PubMed: 16289420]
8. Levin AD, Vukmirovic N, Hwang CW, Edelman ER. Specific binding to intracellular proteins determines arterial transport properties for rapamycin and paclitaxel. Proc Natl Acad Sci U S A 2004;101:9463–9467. [PubMed: 15197278]
9. Herdeg C, Oberhoff M, Baumbach A, Blattner A, Axel DI, Schroder S, Heinle H, Karsch KR. Local paclitaxel delivery for the prevention of restenosis: biological effects and efficacy in vivo. Journal of the American College of Cardiology 2000;35:1969–1976. [PubMed: 10841250]
10. Drachman DE, Edelman ER, Seifert P, Groothuis AR, Bornstein DA, Kamath KR, Palasis M, Yang D, Nott SH, Rogers C. Neointimal thickening after stent delivery of paclitaxel: change in composition and arrest of growth over six months. Journal of the American College of Cardiology 2000;36:2325–2332. [PubMed: 11127480]
11. Creel CJ, Lovich MA, Edelman ER. Arterial paclitaxel distribution and deposition. Circ Res 2000;86:879–884. [PubMed: 10785510]
12. Grube E, Silber S, Hauptmann KE, Mueller R, Buellesfeld L, Gerckens U, Russell ME. TAXUS I: six- and twelve-month results from a randomized, double-blind trial on a slow-release paclitaxel-eluting stent for de novo coronary lesions. Circulation 2003;107:38–42. [PubMed: 12515740]
13. Bullesfeld L, Gerckens U, Muller R, Grube E. Long-term evaluation of paclitaxel-coated stents for treatment of native coronary lesions. First results of both the clinical and angiographic 18 month follow-up of TAXUS I. Z Kardiol 2003;92:825–832. [PubMed: 14579046]
14. Finn AV, Nakazawa G, Joner M, Kolodgie FD, Mont EK, Gold HK, Virmani R. Vascular responses to drug eluting stents: importance of delayed healing. Arterioscler Thromb Vasc Biol 2007;27:1500–1510. [PubMed: 17510464]
15. Lagerqvist B, James SK, Stenestrand U, Lindback J, Nilsson T, Wallentin L. Long-term outcomes with drug-eluting stents versus bare-metal stents in Sweden. N Engl J Med 2007;356:1009–1019. [PubMed: 17296822]
16. Kastrati A, Dibra A, Mehilli J, Mayer S, Pinieck S, Pache J, Dirschinger J, Schomig A. Predictive factors of restenosis after coronary implantation of sirolimus- or paclitaxel-eluting stents. Circulation 2006;113:2293–2300. [PubMed: 16682614]
17. Balakrishnan B, Dooley J, Kopia G, Edelman ER. Thrombus causes fluctuations in arterial drug delivery from intravascular stents. J Control Release 2008;131:173–180. [PubMed: 18713645]
18. Hwang CW, Levin AD, Jonas M, Li PH, Edelman ER. Thrombosis modulates arterial drug distribution for drug-eluting stents. Circulation 2005;111:1619–1626. [PubMed: 15795325]
19. Scheller B, Hehrlein C, Bocksch W, Rutsch W, Haghi D, Dietz U, Bohm M, Speck U. Two year follow-up after treatment of coronary in-stent restenosis with a paclitaxel-coated balloon catheter. Clin Res Cardiol 2008;97:773–781. [PubMed: 18536865]

20. Scheller B, Speck U, Abramjuk C, Bernhardt U, Bohm M, Nickenig G. Paclitaxel balloon coating, a novel method for prevention and therapy of restenosis. Circulation 2004;110:810–814. [PubMed: 15302790]
21. Camenzind E. Treatment of in-stent restenosis--back to the future? N Engl J Med 2006;355:2149–2151. [PubMed: 17101616]
22. Wilensky RL, Mehdi K, Sowinski KM, Baek SH, March KL. Increased Intramural Retention After Local Delivery of Molecules with Increased Binding Properties: Implications for Regional Delivery of Pharmacologic Agents. J Cardiovasc Pharmacol Ther 1999;4:103–112. [PubMed: 10684529]
23. Bratzler RL, Chisolm GM, Colton CK, Smith KA, Zilversmit DB, Lees RS. The distribution of labeled albumin across the rabbit thoracic aorta in vivo. Circ Res 1977;40:182–190. [PubMed: 844144]
24. Ramirez CA, Colton CK, Smith KA, Stemerman MB, Lees RS. Transport of 125I-albumin across normal and deendothelialized rabbit thoracic aorta in vivo. Arteriosclerosis 1984;4:283–291. [PubMed: 6712542]
25. Penn MS, Koelle MR, Schwartz SM, Chisolm GM. Visualization and quantification of transmural concentration profiles of macromolecules across the arterial wall. Circ Res 1990;67:11–22. [PubMed: 2364485]
26. Folch J, Lees M, Sloane Stanley GH. A simple method for the isolation and purification of total lipides from animal tissues. J Biol Chem 1957;226:497–509. [PubMed: 13428781]
27. Allain CC, Poon LS, Chan CS, Richmond W, Fu PC. Enzymatic determination of total serum cholesterol. Clin Chem 1974;20:470–475. [PubMed: 4818200]
28. Wan WK, Lovich MA, Hwang CW, Edelman ER. Measurement of drug distribution in vascular tissue using quantitative fluorescence microscopy. J Pharm Sci 1999;88:822–829. [PubMed: 10430549]
29. Aikawa M, Rabkin E, Voglic SJ, Shing H, Nagai R, Schoen FJ, Libby P. Lipid lowering promotes accumulation of mature smooth muscle cells expressing smooth muscle myosin heavy chain isoforms in rabbit atheroma. Circ Res 1998;83:1015–1026. [PubMed: 9815149]
30. Moller JC, Klein MA, Haas S, Jones LL, Kreutzberg GW, Raivich G. Regulation of thrombospondin in the regenerating mouse facial motor nucleus. Glia 1996;17:121–132. [PubMed: 8776579]
31. Poynton, C. Digital video and HDTV: Algorithms and Interfaces. Morgan Kaufmann; 2003.
32. Balakrishnan B, Dooley JF, Kopia G, Edelman ER. Intravascular drug release kinetics dictate arterial drug deposition, retention, and distribution. J Control Release 2007;123:100–108. [PubMed: 17868948]
33. Balakrishnan B, Tzafriri AR, Seifert P, Groothuis A, Rogers C, Edelman ER. Strut position, blood flow, and drug deposition: implications for single and overlapping drug-eluting stents. Circulation 2005;111:2958–2965. [PubMed: 15927969]
34. Kolachalama VB, Tzafriri AR, Arifin DY, Edelman ER. Luminal flow patterns dictate arterial drug deposition in stent-based delivery. J Control Release 2009;133:24–30. [PubMed: 18926864]
35. Rogers C, Edelman ER. Pushing drug-eluting stents into uncharted territory: simpler than you think--more complex than you imagine. Circulation 2006;113:2262–2265. [PubMed: 16702484]
36. Holmes DR Jr, Kereiakes DJ, Laskey WK, Colombo A, Ellis SG, Henry TD, Popma JJ, Serruys PW, Kimura T, Williams DO, Windecker S, Krucoff MW. Thrombosis and drug-eluting stents: an objective appraisal. J Am Coll Cardiol 2007;50:109–118. [PubMed: 17616294]
37. Tepe G, Zeller T, Albrecht T, Heller S, Schwarzwalder U, Beregi JP, Claussen CD, Oldenburg A, Scheller B, Speck U. Local delivery of paclitaxel to inhibit restenosis during angioplasty of the leg. N Engl J Med 2008;358:689–699. [PubMed: 18272892]
38. Rogers C, Welt FG, Karnovsky MJ, Edelman ER. Monocyte recruitment and neointimal hyperplasia in rabbits. Coupled inhibitory effects of heparin. Arterioscler Thromb Vasc Biol 1996;16:1312–1318. [PubMed: 8857930]
39. Welt FG, Edelman ER, Simon DI, Rogers C. Neutrophil, not macrophage, infiltration precedes neointimal thickening in balloon-injured arteries. Arterioscler Thromb Vasc Biol 2000;20:2553–2558. [PubMed: 11116052]

40. Welt FG, Tso C, Edelman ER, Kjelsberg MA, Paolini JF, Seifert P, Rogers C. Leukocyte recruitment and expression of chemokines following different forms of vascular injury. Vasc Med 2003;8:1–7. [PubMed: 12866605]
41. Bauriedel G, Jabs A, Kraemer S, Nickenig G, Skowasch D. Neointimal Expression of Rapamycin Receptor FK506-Binding Protein FKBP12: Postinjury Animal and Human In-Stent Restenosis Tissue Characteristics. J Vasc Res 2007;45:173–178. [PubMed: 17962721]
42. Weidinger FF, McLenachan JM, Cybulsky MI, Fallon JT, Hollenberg NK, Cooke JP, Ganz P. Hypercholesterolemia enhances macrophage recruitment and dysfunction of regenerated endothelium after balloon injury of the rabbit iliac artery. Circulation 1991;84:755–767. [PubMed: 1713536]
43. Welt FG, Rogers C. Inflammation and restenosis in the stent era. Arterioscler Thromb Vasc Biol 2002;22:1769–1776. [PubMed: 12426203]
44. Tzafriri AR, Levin AD, Edelman ER. Diffusion-limited binding explains binary dose response for local arterial and tumour drug delivery. Cell Prolif 2009;42:348–363. [PubMed: 19438899]
45. Farb A, Heller PF, Shroff S, Cheng L, Kolodgie FD, Carter AJ, Scott DS, Froehlich J, Virmani R. Pathological analysis of local delivery of paclitaxel via a polymer-coated stent. Circulation 2001;104:473–479. [PubMed: 11468212]
46. Zohlnhofer D, Klein CA, Richter T, Brandl R, Murr A, Nuhrenberg T, Schomig A, Baeuerle PA, Neumann FJ. Gene expression profiling of human stent-induced neointima by cDNA array analysis of microscopic specimens retrieved by helix cutter atherectomy: Detection of FK506-binding protein 12 upregulation. Circulation 2001;103:1396–1402. [PubMed: 11245643]
47. Pires NM, Eefting D, de Vries MR, Quax PH, Jukema JW. Sirolimus and paclitaxel provoke different vascular pathological responses after local delivery in a murine model for restenosis on underlying atherosclerotic arteries. Heart 2007;93:922–927. [PubMed: 17449502]
48. Sirianni RW, Kremer J, Guler I, Chen YL, Keeley FW, Saltzman WM. Effect of extracellular matrix elements on the transport of paclitaxel through an arterial wall tissue mimic. Biomacromolecules 2008;9:2792–2798. [PubMed: 18785771]
49. Schwartz RS, Edelman ER, Carter A, Chronos N, Rogers C, Robinson KA, Waksman R, Weinberger J, Wilensky RL, Jensen DN, Zuckerman BD, Virmani R. Drug-eluting stents in preclinical studies: recommended evaluation from a consensus group. Circulation 2002;106:1867–1873. [PubMed: 12356643]
50. Schwartz RS, Edelman E, Virmani R, Carter A, Granada JF, Kaluza GL, Chronos NAF, Robinson KA, Waksman R, Weinberger J, Wilson GJ, Wilensky RL. Drug-Eluting Stents in Preclinical Studies: Updated Consensus Recommendations for Preclinical Evaluation. Circ Cardiovasc Intervent 2008;1:143–153.

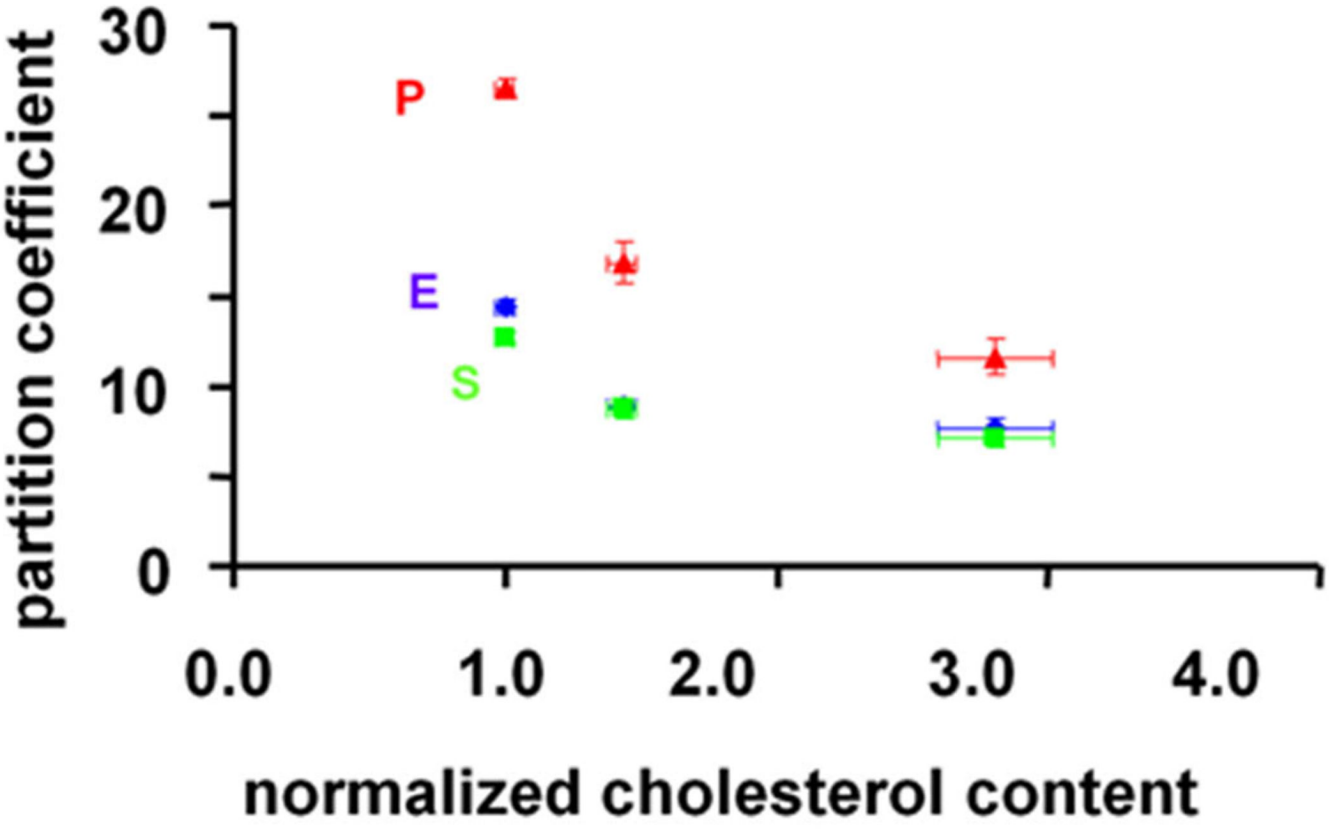

Figure 1.
The partition coefficients (n=3) of everolimus (10 μM, blue), paclitaxel (10 nM, red) and sirolimus (10 μM, green) decrease with increasing cholesterol content (defined as the sum of free and esterified cholesterol, n=3). These data were obtained from a single 3mm thick human aorta sample that was separated into its three tunica layers. Each layer was then cut into 12 square segments (4mm×4mm); 3 for cholesterol quantification and 9 for drug quantification.

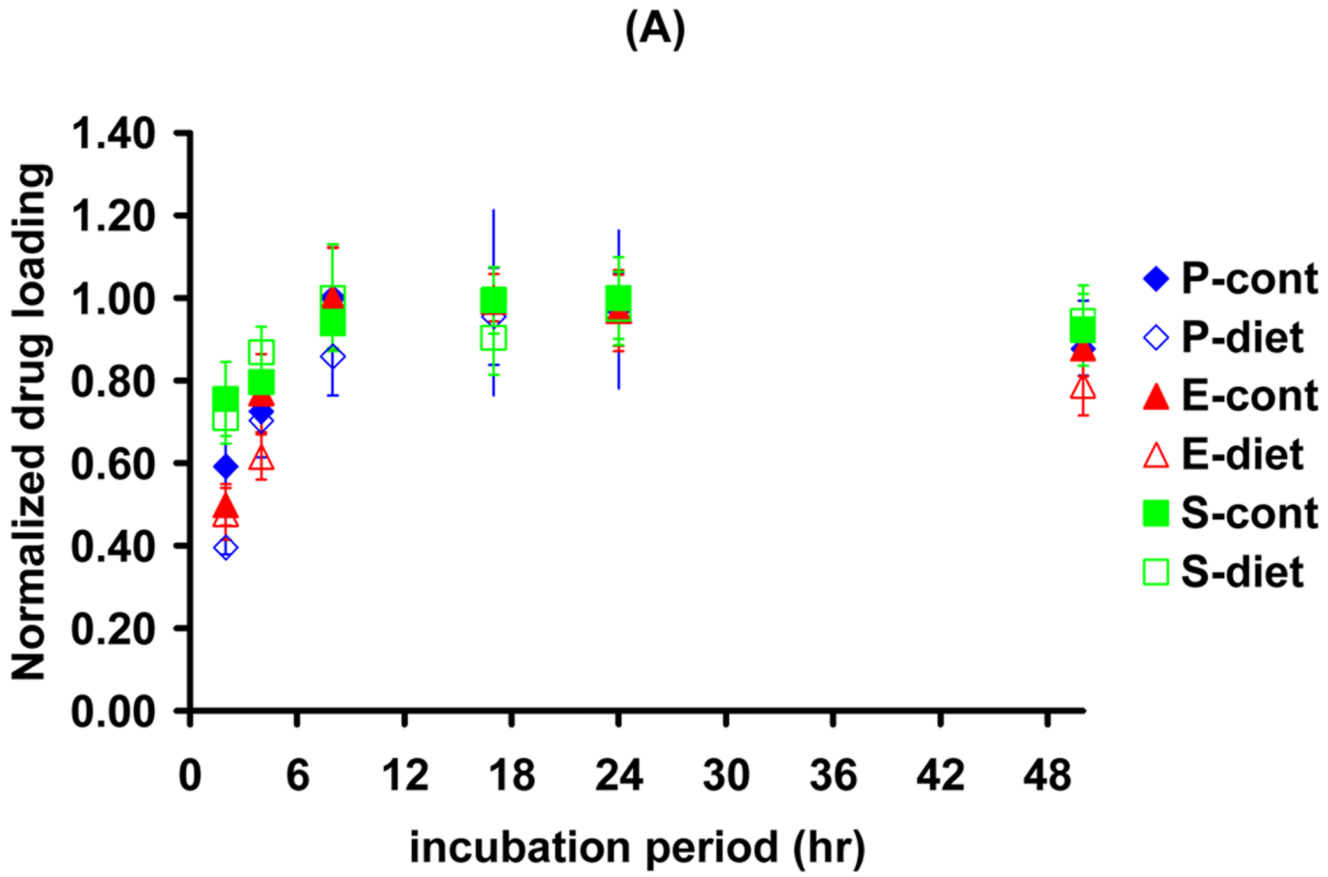

Fig 2A

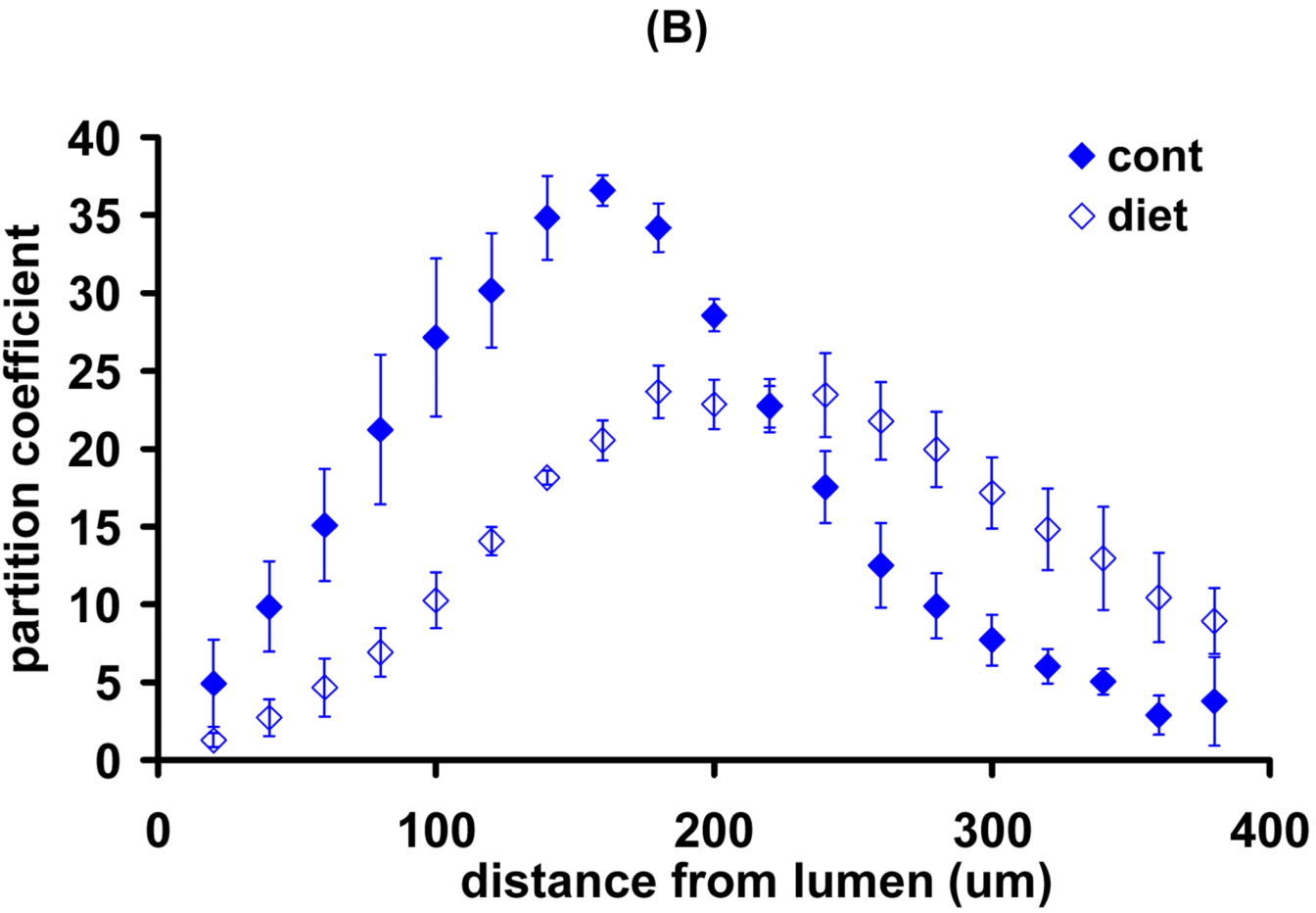

Fig 2B

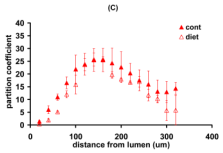

Fig 2C

Figure 2.

Drug absorption and transmural distribution in atheromatous rabbit aortae. (A) The kinetics of net arterial partitioning for control (injured + normal diet, n=3) and atheromatous (injured + cholesterol/oil diet, n=3) samples are independent of tissue state and statistically indistinguishable for paclitaxel (blue), everolimus (red) and sirolimus (green). A second subset of equilibrium incubated arteries was cryosectioned and the partition coefficient

evaluated in 0.020 mm sections (n=3), from the luminal to the adventitial side. Disease state altered the distribution profile of paclitaxel (B) but not of everolimus (C).

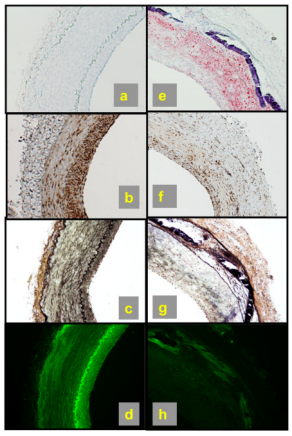

Figure 3.

Arterial ultrastructure determines drug distribution. Control or atherosclerotic arteries were incubated for 24h in fluorescent drug, serial sectioned and either analyzed for compositional distribution or imaged en face using a fluorescent microscope to determine drug distribution. (a,e) oil-red-O stain for lipid. (b,f) tubulin immunostain in brown; (c,g) VerHoeff stain shows elastin as black wavy lines; (d,h) fluorescent paclitaxel deposition (green). Diet and injury decreased total elastin and tubulin levels by 40±5% and 37±5%, respectively. Concomitantly, total fluorescent paclitaxel deposition dropped 73±9% and total lipid levels increased by 28±7%.

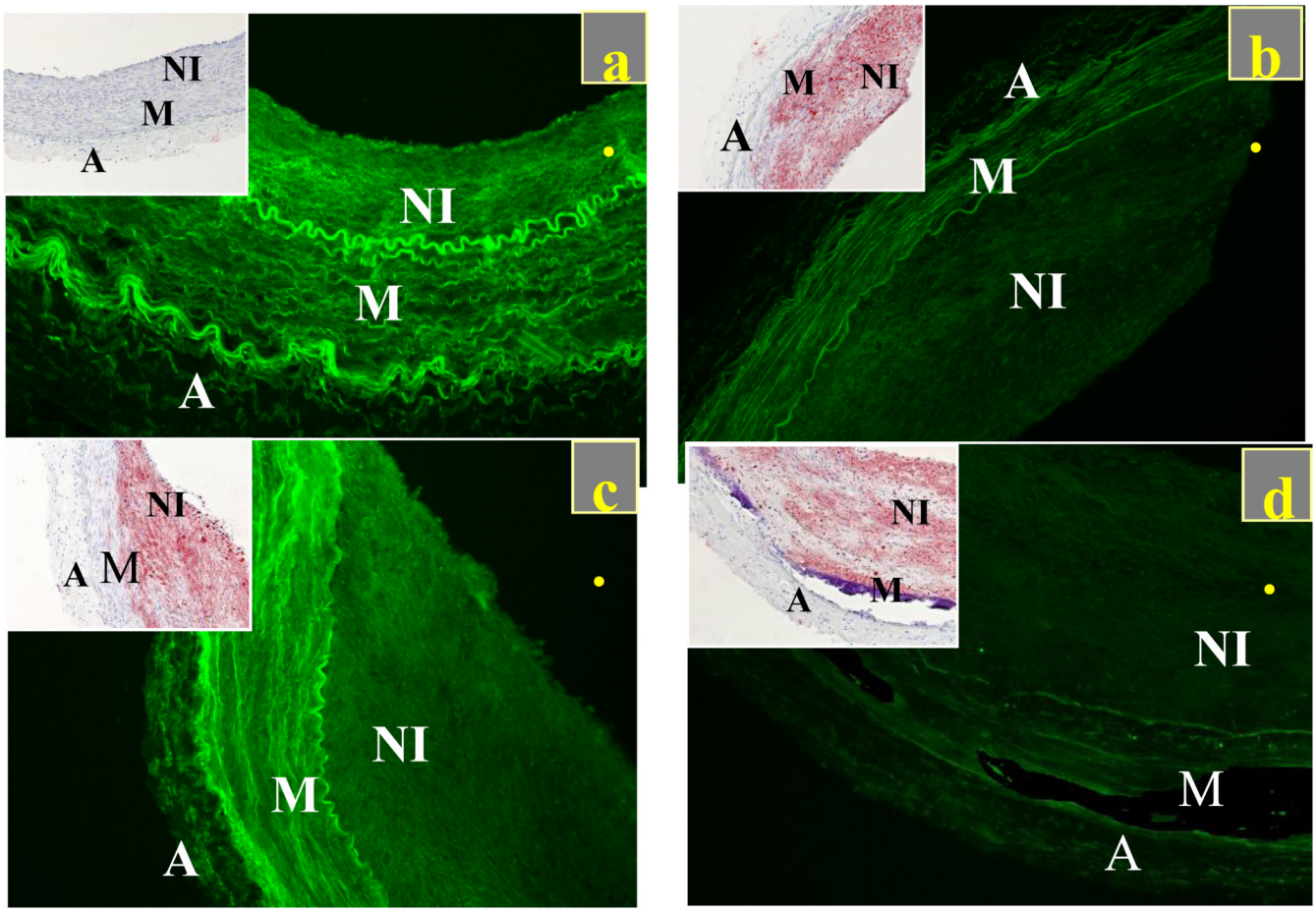

Figure 4.
Local paclitaxel deposition scales inversely with lipid content in control (injury+normal diet, n=2) and diseased arteries (injury + cholesterol/oil diet+normal diet, n=2). Fluorescent paclitaxel (green) and lipid (inset, red) distribution in control artery (a) and in lesions of varying complexity (b)–(d). All samples imaged at the same intensity level and processed to eliminate backgrounds and artifacts with minimal residual autofluorescence exhibited by control arteries that were incubated in PBS (supplemental figure S2).

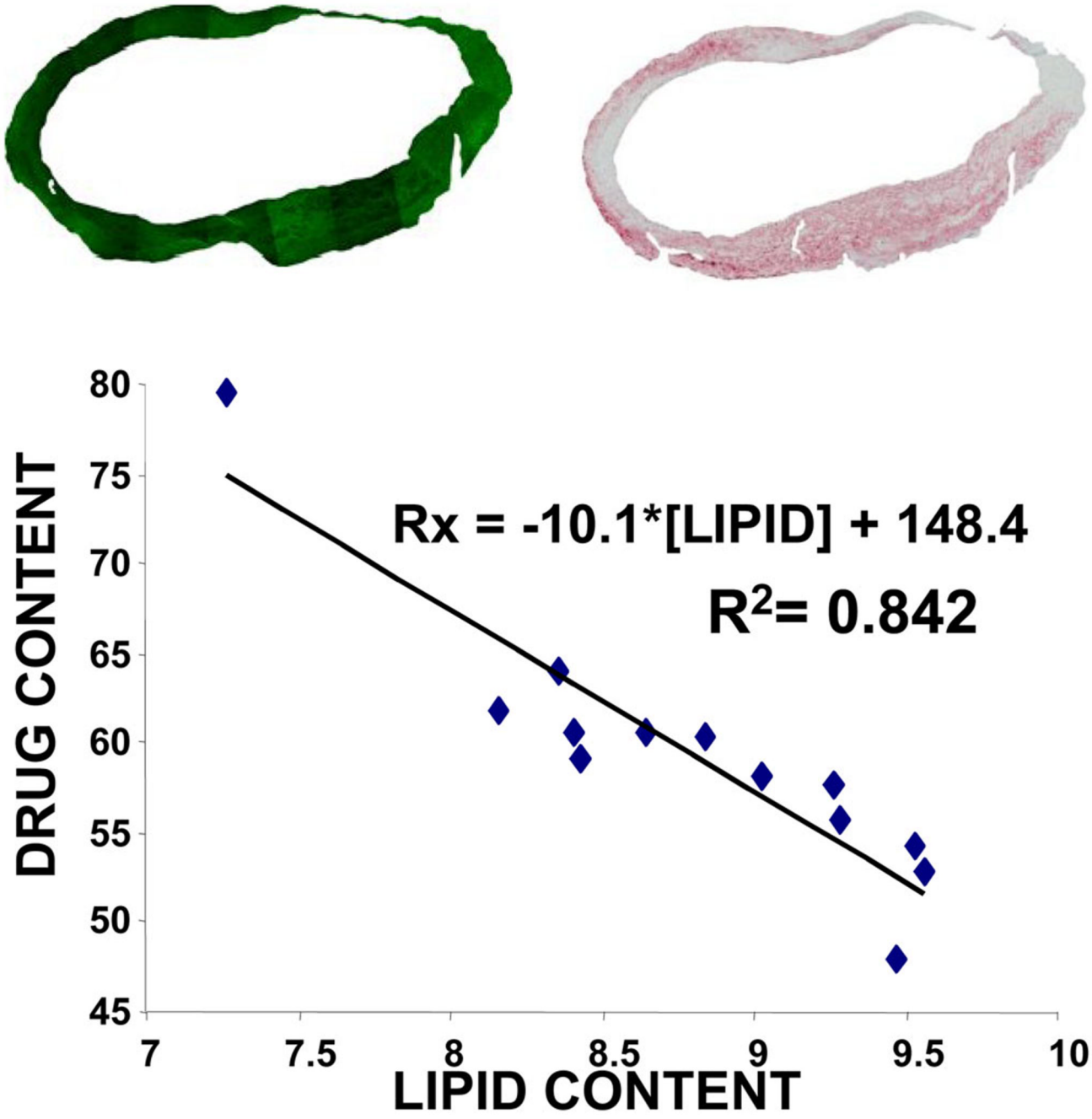

Figure 5.

(Top) Images of neointima with fluorescent paclitaxel deposition in green (left) and Oil-Red-O stain for lipid in red (right) were processed to eliminate backgrounds and artifacts. Pixel luminosities relative to threshold values were extracted for all zones of interest, and their percentage taken as a measure of drug and lipid contents. (Bottom) Analysis of multiple sectors converged to an inverse linear correlation (R^2=0.842) between drug content and lipid content per section, the more lipid in the section the less drug. Circumferential irregularities in tissue fluorescence (top) arise from unavoidable variations in tissue processing and account for the spread in fluorescent intensity that arises from tissue regions that express at high levels of lipid.